

# Jeopardy Proposal for the Remaining Six Days of the g3 Experiment

Original Experiments:

91-014: Quasi-Free Strangeness Production in Nuclei

93-008: Inclusive Eta Photoproduction in Nuclei

93-044: Photoreactions on  $^3\text{He}$

Updated g3 Collaboration:

B.L. Berman,\*# Y.Y. Ilieva,\* N. Benmouna, C. Bennhold, W.J. Briscoe, G. Feldman,  
P. Heimberg, S. Niccolai, I.I. Strakovsky, and S. Strauch  
The George Washington University

M.F. Vineyard\*  
Union College

I. Niculescu\* and K. Giovanetti  
James Madison University

G. Audit and J-M. Laget  
CEA Saclay

M. Anghinolfi, M. Battaglieri, R. De Vita, G. Ricco, M. Ripani, and M. Taiuti  
INFN Genova

G. Niculescu  
Ohio University

G.V. O'Rielly  
University of Massachusetts at Dartmouth

G.P. Gilfoyle  
University of Richmond

H.L. Crannell and D.I. Sober  
Catholic University of America

J.W. Jury, C. Hourie, and D. McCallum  
Trent University

and the CLAS Collaboration

\*Co-spokesperson

#Contact person

E-mail: [berman@gwu.edu](mailto:berman@gwu.edu)

Phone: (202) 994-7192; Fax: (202) 994-3001

# Jeopardy Proposal for the Remaining Six Days of the g3 Experiment

## Proposed Experiment on $^{12}\text{C}$ and Its Extension to Pb

The g3 group of experiments was approved for 25 days of beam time—13 days for  $^3\text{He}$  and 6 days each for  $^4\text{He}$  and  $^{12}\text{C}$ . The  $^3\text{He}$  part was run in December 1999, and was so successful that we were able to use the last part of this scheduled time (g3a) to perform the  $^4\text{He}$  part of the experiment as well. Thus, at the cost of only about half of the approved beam time, about  $\frac{3}{4}$  of the experimental data have been obtained.

There remains the  $^{12}\text{C}$  part (g3b) to be completed, and this is what we currently propose to do. However, because we found in our earlier run that we were able to take data at a rate greater than that originally anticipated, we would like to add a foil of  $^{\text{Nat}}\text{Pb}$  to the carbon (graphite) foils in our target and obtain data on this heavy nuclear target simultaneously with those on our  $^{12}\text{C}$  target. We compute (see below) that by apportioning our counting rates in the ratio of roughly  $^{12}\text{C}:\text{Pb} = 2:1$ , we can obtain the required data on both, wholly within the originally approved beam time of 6 days.

The use of the nucleus as a highly-condensed-matter laboratory is an important component of the Jefferson Lab physics program. In it one can study the modification of the elementary amplitudes for many processes by the strongly interacting nuclear medium. At the present time, we have obtained an enormous amount of real-photon data on the proton (g1) and a large amount on the deuteron (g2) as well, from which one can extract the elementary amplitudes on the proton and the neutron. As we are now seeing from the ongoing analysis of the g3a data (see below), we have ample data on  $^3\text{He}$  and  $^4\text{He}$  as well. What is lacking, obviously, are data on heavier nuclei.

The binding energy per nucleon, mean radius, and density for  $^2\text{H}$ ,  $^3\text{He}$ ,  $^4\text{He}$ ,  $^{12}\text{C}$ , and  $^{208}\text{Pb}$  are given in the following table:

Nucleus	Binding energy per nucleon (MeV)	Mean radius (fm)	Density (nucleons per cubic fm)
$^2\text{H}$	1.11	2.0	0.06
$^3\text{He}$	2.57	1.8	0.12
$^4\text{He}$	7.07	1.6	0.23
$^{12}\text{C}$	7.68	2.3	0.24
$^{208}\text{Pb}$	7.86	~6.0	0.23

It is clear from these values that if we wish to study the density dependence of an interaction, we should compare the data for  $^2\text{H}$ ,  $^3\text{He}$ , and  $^4\text{He}$ , whose sizes are not very different but whose densities vary by a factor of about 4. This we are already doing, using the data from g2 and g3a. But if we wish to study the size dependence of an interaction, we should compare data for  $^4\text{He}$ ,  $^{12}\text{C}$ , and Pb, whose densities (or binding energies/nucleon) are about the same, but whose radii vary by a factor of about 4. An example where density dependence is our prime concern is the issue of three-body forces,

whose range is much shorter than two-body forces, and whose study therefore requires that the incoming short-wavelength photon interact with the three nucleons when they are close together. We can carry out such studies with our existing data. But for those interactions the study of which depends critically on the mean free path of a particle in nuclear matter, such as the interaction of photoproduced kaons, etas, or Deltas with nucleons, we require data obtained with larger target nuclei.

### **g3 Data Analysis to Date (S. Niccolai and others)**

The g3 run group of experiments ran for about three weeks in December, 1999. We obtained data over the full range of the Photon Tagger—0.33 to 1.56 GeV with an incident electron-beam energy of 1.645 GeV. Tagged, circularly polarized photons, produced by the 70% longitudinally polarized electrons, were incident on liquid-helium targets positioned at the center of the CLAS. This was the first experiment to use a second-level trigger, and we were able to collect data at rates exceeding 3 kHz. We succeeded in collecting approximately 1.2 billion events for  $^3\text{He}$  and 0.8 billion for  $^4\text{He}$ .

A small part of the data (a few million events) were analyzed with existing calibrations; they show (see below) that the main goals of the experiment have been reached: we do indeed have sufficient data for the principal reaction channels of interest.

Progress since then has been concentrated in four areas:

- Normalization procedures for the tagged-photon flux have been studied at length. After the two main techniques used previously were shown to give results generally within 5%, the data are now being processed with the new “gflux” technique.
- Calibration studies revealed certain problems with the time-of-flight counters for sectors 3 and 4, which have now been accounted for.
- Data transfer to the new GW mass-storage facility (our “minisilo”), for eventual cooking and analysis by the new GW computer cluster (our “minifarm”), was very slow, because of difficulties encountered in the transfer of a data set of this magnitude (about 5.5 Tb), but has now been completed.
- Pass-zero cooking (the first file of each data run, comprising between 5 and 10% of the total) was completed, and showed generally very good stability throughout the running period.
- Pass-one cooking (the first pass for the complete data set) is now underway, and is about 50% complete.

Figures 1 and 2 illustrate the data on the three-body breakup channel of  $^3\text{He}$ . Figure 1 shows the striking peak in the missing-mass spectrum of two protons just at the mass of the neutron. The distribution of three-body-breakup events on a two-dimensional triangular Dalitz plot (where the energy of each nucleon is plotted perpendicular to one of the sides of an equilateral triangle) shows a large number of “star” events, candidates for three-body-force effects because all three nucleons have approximately the same energy and relative momentum. Figure 2 shows a cut along the neutron-energy axis in the Dalitz plot, showing that a valley exists between the regions dominated by two-body and three-body events, and that the three-body events peak near the symmetric star kinematics.

Figures 3 and 4 illustrate the data on the quasifree Delta production on a nucleon in  $^4\text{He}$ , focusing on  $\Delta^0$  production on a neutron in the nucleus and its subsequent decay into the  $p-\pi^-$  channel. Figure 3 shows the remarkable peak in the  $p-\pi^-$  missing-mass spectrum just at the mass of the (spectator)  $^3\text{He}$ . Figure 4 shows the invariant mass of the events in this peak, showing that most of them occur near the mass of the  $\Delta^0$ . This is the first example of the use of  $^4\text{He}$  as a neutron target.

Various other results from analysis of the g3a data will be shown in subsequent parts of this proposal, as appropriate.

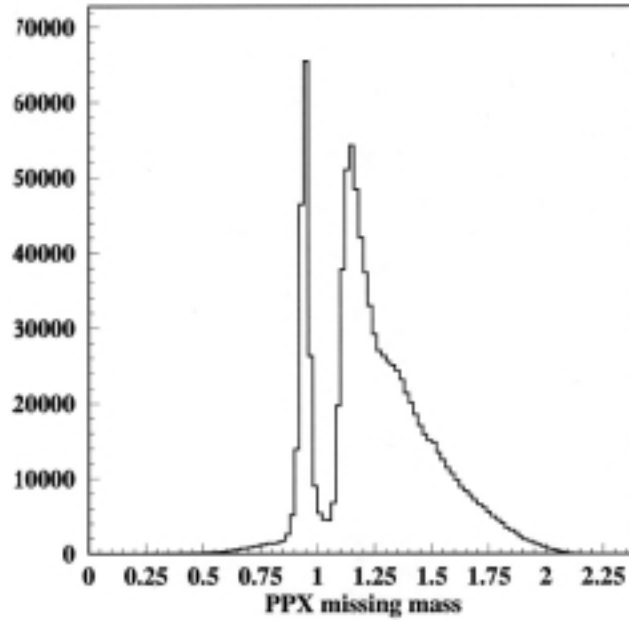


Figure 1. Missing-mass distribution when two protons from the photodisintegration of  $^3\text{He}$  are detected in the CLAS. The narrow peak at the neutron mass ( $0.939 \text{ GeV}/c^2$ ) signals the three-nucleon breakup reaction.

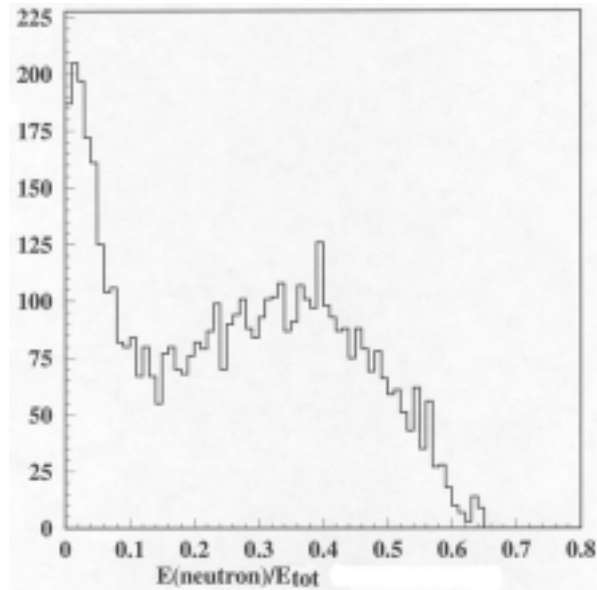


Figure 2. Distribution of neutron energies for those three-nucleon events in which the two detected protons have nearly equal energies. From kinematics,  $E_{\text{nmax}} = 2/3 E_{\text{tot}}$ .

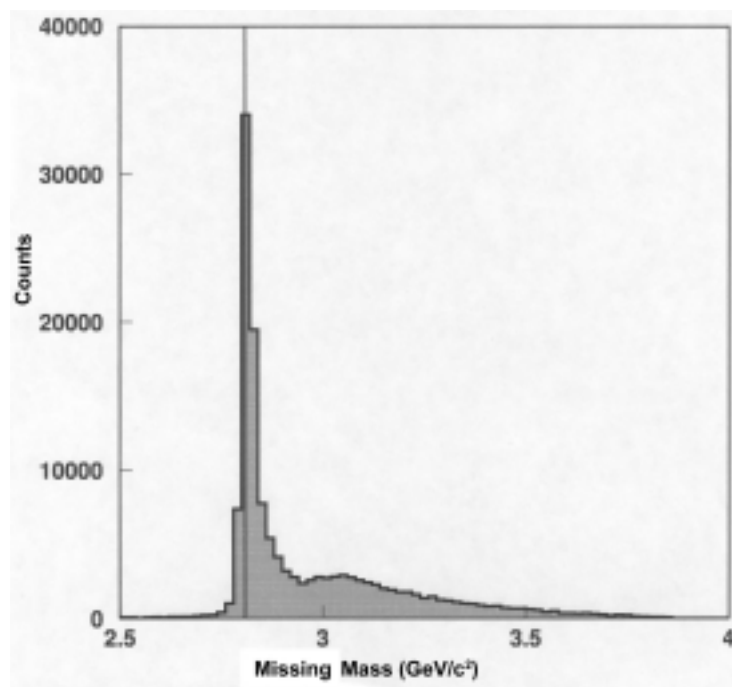


Figure 3. Missing-mass distribution when a proton and a  $\pi^-$  from a photoreaction on  ${}^4\text{He}$  were detected in the CLAS. The peak at the (spectator)  ${}^3\text{He}$  mass indicates the importance of the quasifree pion-production process.

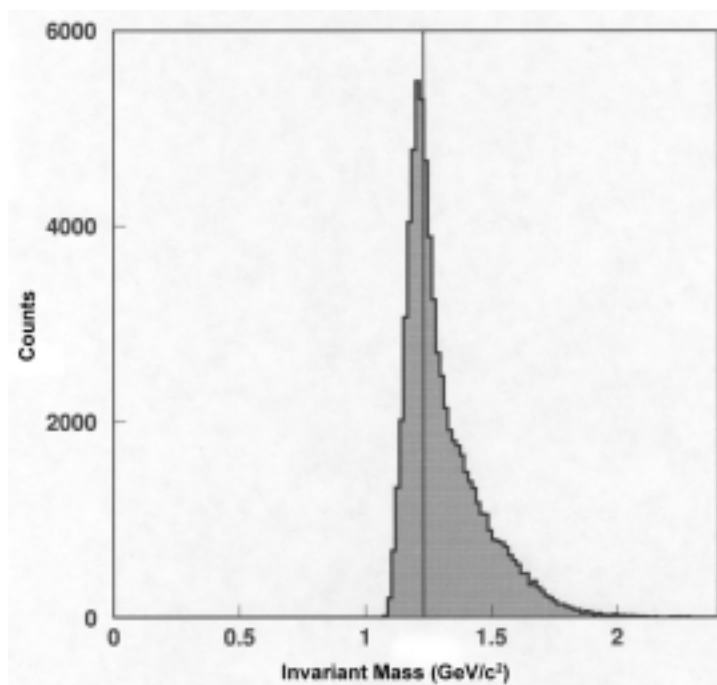


Figure 4. Invariant mass distribution for the quasifree events shown in Fig. 3. The line marks the mass of the  $\Delta^0$ .

## Strangeness Production (I. Niculescu)

Experiment 91-014 encompasses the measurement of strangeness photoproduction in  $^3\text{He}$ ,  $^4\text{He}$ , and  $^{12}\text{C}$ . In addition, we have carried out considerable work on the analysis of the g2 data to extract the photoproduction of the  $\Sigma^-$  hyperon on the neutron; this analysis is now well along, and has only been awaiting the final cooking of the g2 data to be completed. For  $^{12}\text{C}$  and Pb, we intend to extract the A-dependence of the inclusive  $\text{K}^+$  production as well. Since the  $\text{K}^+$  has a relatively long mean free path in the nucleus, it constitutes a unique probe of nuclear matter, which has scarcely been exploited heretofore.

The quasifree kaon-photoproduction reaction in nuclei is governed by three main mechanisms:

- The elementary amplitudes of the six kaon production reactions possible on the nucleon ( $\gamma p \rightarrow \text{K}^+\Lambda$ ,  $\gamma p \rightarrow \text{K}^+\Sigma^0$ ,  $\gamma p \rightarrow \text{K}^0\Sigma^+$ ,  $\gamma n \rightarrow \text{K}^+\Sigma^-$ ,  $\gamma n \rightarrow \text{K}^0\Lambda$ ,  $\gamma p \rightarrow \text{K}^0\Sigma^0$ ).
- The Fermi motion of the proton and neutron inside the nucleus.
- The interaction between the final-state hadrons.

Experimental information exists for the first three exclusive kaon photoproduction channels [Tra98], [Ben98] and results for the  $\gamma n \rightarrow \text{K}^+\Sigma^-$  from the deuteron (g2) will become available soon [Nic01]. Electromagnetic production of strangeness is complementary to hadron-induced reactions [Dov91]. In a quasifree reaction the interaction is considered to take place on a single nucleon, thus making this type of reaction a good tool to study the propagation of hadrons in the nuclear medium. The photon can penetrate deep inside the nucleus, producing only minimal distortions to the initial state.  $\text{K}^+$  and  $\text{K}^0$  photoproduction data on nuclear targets can thus be used to probe the exclusive  $\text{N}(\gamma, \text{K})\Lambda, \Sigma$  vertex functions in the nuclear medium [Hyd91].

Recent theoretical studies have investigated the possibility of using quasifree kaon photoproduction to probe the hyperon-nucleon interaction [Lee01], [Abu00]. Polarization observables (recoil polarization of the  $\Lambda$  hyperon and the photon asymmetry) in quasifree kaon photoproduction are shown to be almost independent of the target nucleus and insensitive to relativistic effects [Abu00]. Thus, such measurements are ideally suited for probing in-medium modifications of the elementary amplitudes. In the left panel of Fig. 5 the recoil polarization of the  $\Lambda$  hyperon is shown as a function of the kaon scattering angle for a few nuclei; the results on the free proton are also shown. While the recoil polarization in nuclei is different than on the free proton, this observable is predicted to have practically no dependence on the target nucleus; this prediction calls for an experimental test. For completeness, the right panel of Fig. 5 shows the beam asymmetry.

$\text{K}^+$  mesons interact only weakly with the nuclear medium, thus preserving the information about the production mechanism relatively undisturbed. This feature is essential in the study of in-medium self energies of kaons, presently discussed in the framework of heavy-ion collisions [Sib01]. Figure 6 shows the effects of the final-state interactions under quasifree kinematics in carbon. The three vertical panels correspond

to the  $K^+\Lambda$ ,  $K^+\Sigma^0$ , and  $K^+\Sigma^-$  production. From top to bottom are shown the differential cross section, the beam asymmetry, and the hyperon recoil polarization. For each panel, the different curves show the predictions of a PWIA calculation (no FSI)—dashed line, DWIA with only kaon FSI—dotted line, DWIA with only hyperon FSI—dash-dotted line, and the full DWIA—solid line. While the differential cross section shows the most sensitivity to FSI, for each of these channels there is at least one polarization observable almost impervious to the effects of the FSI.

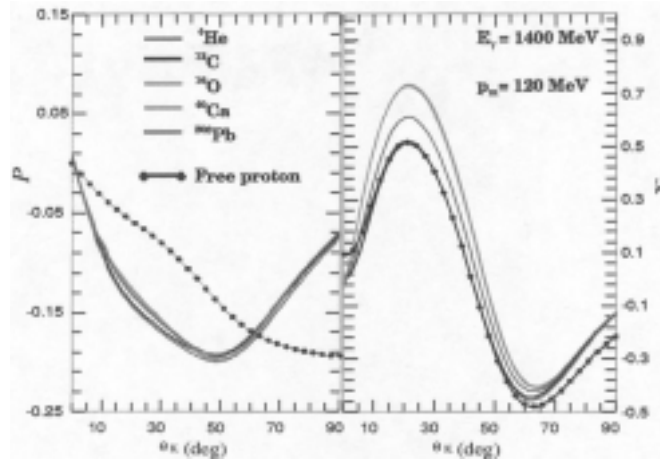


Figure 5. Recoil polarization of the  $\Lambda$  hyperon (left) and the photon asymmetry (right) as a function of the kaon scattering angle for the proton and various nuclei (from [Abu00]).

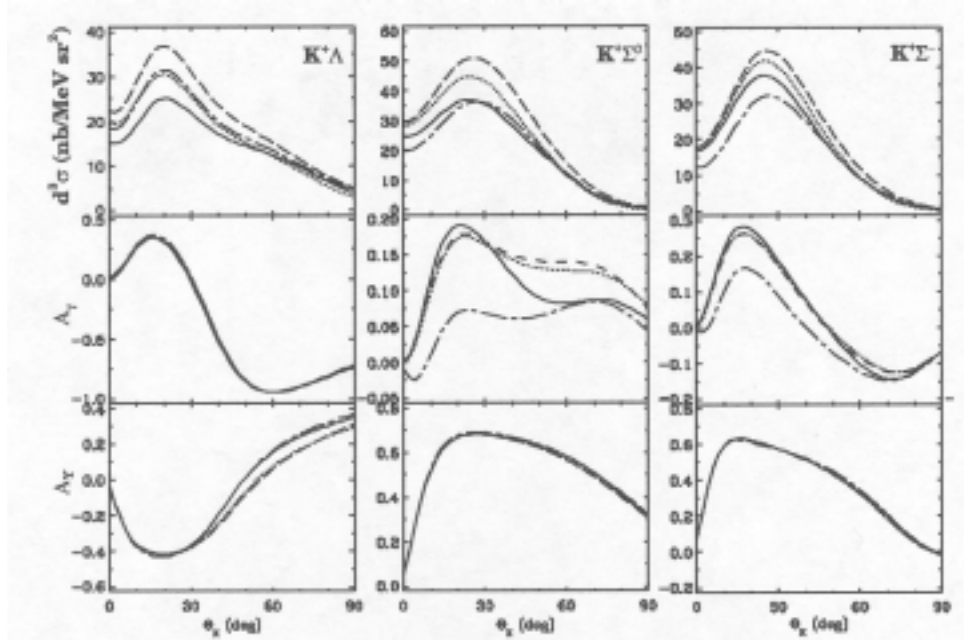


Figure 6. Differential cross section (top), beam asymmetry (middle), and hyperon recoil polarization (bottom) as a function of the kaon angle (from [Lee01], modified). See text for explanation of the curves shown.

With the advent of high-duty-cycle, high-intensity electron accelerators, experimental information has started to become available. Kaon electro- and photoproduction data on deuterium,  $^3\text{He}$ , and  $^4\text{He}$  have been obtained at Jefferson Lab. However, there is still very little experimental information available for heavier nuclei [Yam95].

The data on deuterium (from g2—the  $^3\text{He}$  and  $^4\text{He}$  data from g3a are currently being analyzed) were used to extract cross sections for  $\Sigma^-$  photoproduction on the neutron. In this analysis the reaction  $\gamma n \rightarrow K^+ \Sigma^-$  was selected by detecting the positive kaon and the decay products of the  $\Sigma^-$ , the neutron and the negative pion [Nic01]. This analysis is approaching completion, currently going through the peer-review process in Hall B. A similar technique can be used to extract the  $\Sigma^-$  contribution for heavier targets. The CLAS capability of detecting multiparticle final states thus presents an advantage over similar experiments that detect only the outgoing kaon [Zei01]. The availability of circularly polarized photons also enables us to access important polarization observables.

The main challenges of measuring hyperon electromagnetic production cross sections are the detection of the kaon and the identification of the reaction channel. Figure 7 shows the technique used in the  $^3\text{He}$  analysis; a similar procedure will be followed for the carbon and lead targets. The top left panel shows the time-of-flight mass of the kaon candidates, before and after tightening the PID cuts (see [Nic01] for more details). The top right panel shows the invariant mass of the  $p\pi^-$  system detected in coincidence with the emerging kaon. One sees a narrow peak corresponding to the mass of the  $\Lambda$  hyperon. The bottom left panel of Fig. 7 shows the invariant mass of the  $n\pi^-$  system; the sharp structure seen corresponds to the  $\Sigma^-$  events produced on the neutron. The bottom right panel of Fig. 7 represents the missing mass recoiling against the  $K^+$  meson, only for the events in which a proton and a  $\pi^-$  were also detected. The two vertical lines correspond to the  $\Lambda$  and the  $\Sigma^0$  thresholds.

The proposed experiment will measure quasifree kaon photoproduction on carbon and lead targets. The beam asymmetry with circularly polarized photons and the hyperon recoil polarization will be studied as a function of the target nucleus. The experiment should be able to provide a measurement of the  $\Lambda$ -to- $\Sigma^0$  ratio in nuclei, as well as data on the  $\Sigma^-$  production on bound neutrons. Rate estimates based on published cross-section data [Yam95] as well as the current CLAS analysis of the  $^3\text{He}$  data (expected photon flux, acceptance, *etc.*) indicate that the detection of about 100 fully reconstructed events per hour should be possible for a  $1\text{-g/cm}^2$  thick target. Of course, for kaon inclusive events, the rates are significantly higher.

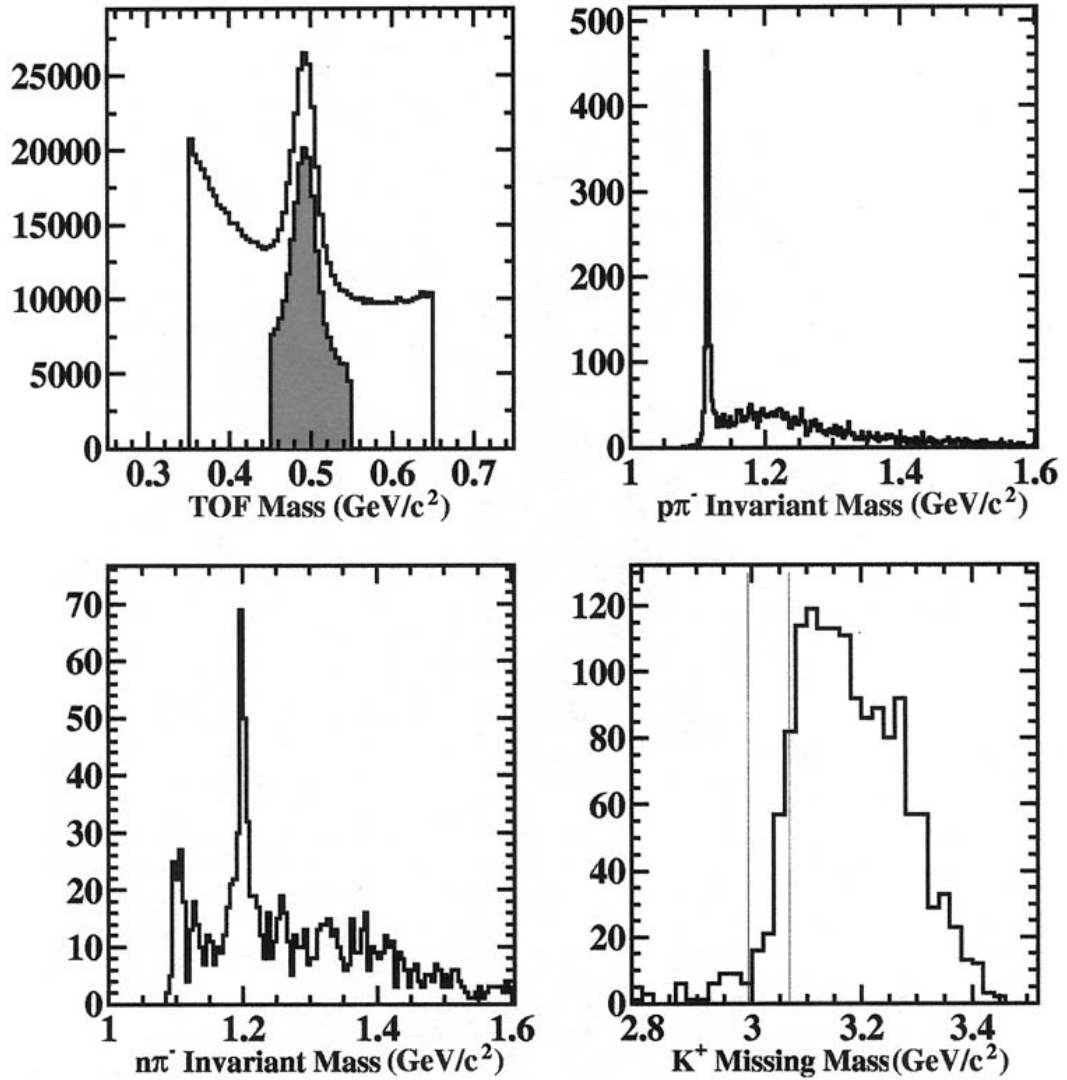


Figure 7. Illustration of the major analysis steps of the  $^3\text{He}$  strangeness photoproduction data obtained with the CLAS. [The mass units are  $\text{GeV}/c^2$ .] See text for details.

## Eta Production (M.F. Vineyard)

Experiment 93-008 encompasses the measurement of inclusive  $\eta$  photoproduction in nuclei, and is part of both the g2 and g3 run groups. Its primary motivation is to investigate nuclear-medium modifications of nucleon resonances and the  $\eta$ -nucleon interaction.

Through the study of the excitation, propagation, and decay of nucleon resonances in the nuclear environment, one ultimately expects to understand how the strong interaction is affected by baryon structure. Over the last twenty-five years, a wealth of information on the  $\Delta(1232)$  and its dynamics within the nuclear medium has been obtained through pion studies. However, very little is known about medium properties of the higher-energy excited states of the nucleon. This is primarily due to the fact that the dominance of the  $\Delta$  and the overlapping of higher resonances prevents the study of only a single specific state by  $\pi$ -production experiments. The  $\eta$  meson, on the other hand, couples only with isospin- $\frac{1}{2}$   $N^*$  resonances since it is an isoscalar particle, and therefore provides an excellent way to isolate these resonances. In this experiment, inclusive measurement of the photoproduction of  $\eta$  mesons in nuclei are performed to investigate medium modifications of the  $S_{11}(1535)$  and possibly other isospin- $\frac{1}{2}$  resonances.

These measurements will also provide information on the  $\eta$ -nucleus interaction. Due to the lack of  $\eta$  beams, very little is known about the interaction of  $\eta$  mesons with nuclei. In this experiment, final-state interactions of the  $\eta$  meson propagating through the nucleus will be used to investigate the  $\eta$ -nucleus interaction. The study of  $\eta$  interactions with nucleons and nuclei can provide significant tests of our understanding of meson interactions which has been developed through pion studies.

A somewhat more speculative motivation for the experiment is to search for the possible formation of  $\eta$ -nucleus bound states. Such states were predicted [Hai86] to exist in nuclei with  $A \geq 12$  and have widths of approximately 9 MeV. Subsequent theoretical work [Chi91] indicates that the widths in these nuclei could be much larger. Other theoretical studies [Wil93], [Wyc95], [Rak96], [Gre96] suggest the possibility of forming  $\eta$ -nucleus bound states even in very light nuclei ( $A = 2, 3, 4$ ). Early experimental searches for these states using pion-induced reactions [Chr88], [Lie89] yielded negative results. However, data from a recent photoproduction experiment at the 1-GeV Lebedev synchrotron [Sok01] are suggestive of the formation of  $\eta$ -mesic nuclei. The experimental signature for the existence of these states would be a peak in the proton spectrum at forward angles when a coincidence is required with conjugate  $\pi^-$ -proton pairs from the decay of the  $\eta$ -mesic nucleus. Since this reaction requires detection of a three-particle coincidence, the CLAS detector is an ideal tool to investigate this final state.

Data were obtained several years ago at MAMI for the inclusive reaction on  $^{12}\text{C}$ ,  $^{40}\text{Ca}$ ,  $^{93}\text{Nb}$ , and  $^{\text{Nat}}\text{Pb}$  nuclei for photon energies up to 790 MeV [Roe96]. These data are of high quality; however, the energy range covered is from threshold to just below the

peak of the  $S_{11}(1535)$  resonance. From the analysis of these data, it was concluded that the total cross section scales as  $A^{2/3}$ , and a Glauber-model analysis indicated an  $\eta$ -N cross section of about 30 mb. No evidence of a shift in mass or a depletion of strength of the  $S_{11}(1535)$  was observed from a comparison with an effective-Lagrangian model [Car93]. However, it should be stressed that this conclusion was drawn from a comparison of the slopes of the data and calculations on the low-energy side of the  $S_{11}(1535)$  rather than over the entire line shape of the resonance.

Recently, the  $^{12}\text{C}(\gamma, \eta)$  reaction was investigated at photon energies between 0.68 and 1.0 GeV at the 1.3-GeV electron synchrotron at KEK-Tanashi [Yor00]. The cross section as a function of incident photon energy was observed to increase with photon energy up to 0.9 GeV and then to begin to decrease. This was interpreted as the first observation of the  $S_{11}(1535)$  resonance in the carbon nucleus. It was shown that some of the differences between the shapes of the cross sections measured on carbon and hydrogen can be accounted for by medium effects such as Fermi motion, Pauli blocking, and  $\eta$ -N and N-N\* collisions in quantum molecular dynamics calculations.

There have been a number of theoretical results on  $\eta$  photoproduction from nuclei in the last decade. In the effective-Lagrangian approach [Car93], the  $\eta$ -N final-state interactions are taken into account by a Monte-Carlo code using calculated reaction probabilities. In the approach of [Lee96], the quasifree production is calculated in the distorted-wave impulse approximation and the final-state interactions are treated with an  $\eta$ -A optical potential. In that of [Eff97], the production cross sections on the free nucleon are used as input and the final-state interactions are taken into account with a coupled-channel model. Recently, a relativistic model has been introduced [Hed98] in which an effective-Lagrangian approach is used to describe the elementary production process and the dynamics of the nucleon motion is based on a relativistic mean-field theory. Several of these models provide reasonable descriptions of the MAMI total cross sections, although detailed agreement with the differential cross sections is not obtained with any of the models. It should be noted, however, that none of these calculations includes any medium modification of the  $S_{11}(1535)$ .

The Jefferson Lab experiment proposed here will extend the MAMI measurements to higher energies. This extended energy range will completely cover the region of the  $S_{11}(1535)$  resonance and allow for a more thorough investigation of possible nuclear-medium modifications. It will also allow for the measurement of contributions to the cross section from other resonances and from nonresonant production. Data are currently being analyzed for  $\eta$  photoproduction on  $^1\text{H}$ ,  $^2\text{H}$ ,  $^3\text{He}$ , and  $^4\text{He}$  targets. Measurements on  $^{12}\text{C}$  and Pb will provide an important overlap with the MAMI results and will enable the study of the evolution of medium effects with target mass and investigation of the  $\eta$ -N interaction.

Shown in Fig. 8 are preliminary invariant-mass spectra for  $\gamma\gamma$  events from hydrogen, deuterium, and  $^3\text{He}$  targets. The spectra are fitted with a function consisting of a quadratic piece to describe the background in the mass region 0-0.23  $\text{GeV}/c^2$  and an exponential part to fit the background at higher mass, and two Gaussians to fit the  $\pi^0$

(mass = 0.135 GeV/c<sup>2</sup>) and  $\eta$  (mass = 0.547 GeV/c<sup>2</sup>) peaks. These spectra represent a small fraction ( $\leq 5\%$ ) of the total data set for each target.

The estimate of the number of  $\eta$  mesons produced on <sup>12</sup>C in this experiment has changed from the original proposal due to the increased data rate that we have achieved since the time the proposal was written, and we now also have better estimates for the cross sections. To estimate the  $\eta$  counting rates on <sup>12</sup>C, we assume a total tagged photon flux of  $2 \times 10^7$  photons/s and energy bins of 100 MeV. The total  $\eta$  photoproduction cross section on <sup>12</sup>C decreases from approximately 65  $\mu\text{b}$  at 0.8 GeV [Roe96] to 10  $\mu\text{b}$  at 1.5 GeV. The cross section at 1.5 GeV was estimated assuming the elementary  $\eta$  photoproduction cross section is 2  $\mu\text{b}$  [Dug02] and that the total cross section scales as  $A^{2/3}$  [Roe96]. Simulations indicate that the acceptance increases from about 4% at 0.8 GeV to 9% at 1.5 GeV. Assuming a target thickness of 1 g/cm<sup>2</sup>, the counting rates decrease from a maximum of 0.092 s<sup>-1</sup> for the 0.8-0.9 GeV energy bin to 0.018 s<sup>-1</sup> for the 1.4-1.5 GeV bin. At these rates we would detect about 50,000 etas in the former and 10,000 in the latter in 150 hours.

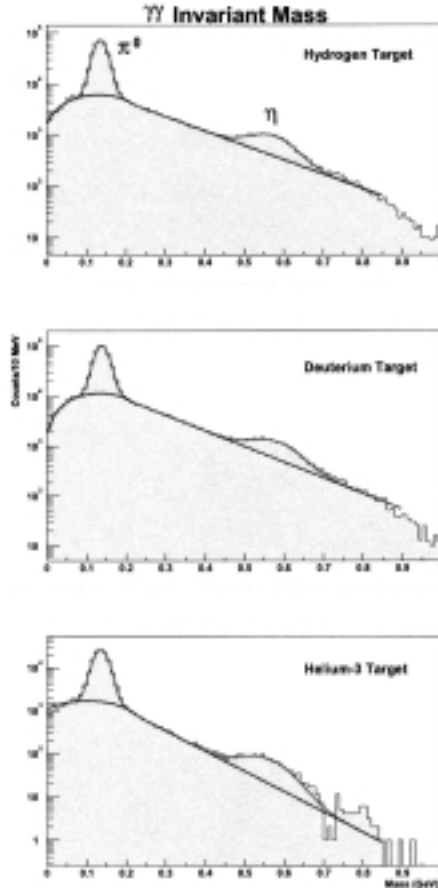


Figure 8. Invariant-mass spectra for  $\gamma\gamma$  events from hydrogen, deuterium, and <sup>3</sup>He targets. The spectra are fitted with a background function and two Gaussian functions. The background function has a quadratic form over the range 0-0.23 GeV/c<sup>2</sup> and an exponential form for mass >0.23 GeV/c<sup>2</sup>. The  $\pi^0$  (mass = 0.135 GeV/c<sup>2</sup>) and  $\eta$  (mass = 0.547 GeV/c<sup>2</sup>) peaks are fitted above the background with the Gaussian functions.

## Delta Knockout (Y.Y. Ilieva)

Experiment 93-044 encompasses three major (and several minor) components. One major component is the study of three-body forces, illustrated above. A second is the study of total photonuclear absorption (see below). The third is the study of the small Delta component in the ground-state wave function of the nucleus, which can be addressed most unambiguously by measuring the direct knockout of the  $\Delta^{++}$ . This is the one of these three subjects that we believe to be the most promising for the present proposal.

The importance of the experimental determination of the  $\Delta$ -isobar component in the nuclear ground state as a test of various theoretical descriptions of nuclear dynamics, especially short-range effects and predictions of the binding energy and magnetic moment, was emphasized in the original 93-044 proposal. Here we will demonstrate the reliability of the experimental data and the method of data analysis already applied to  ${}^3\text{He}$ .

We search for clear evidence of a pre-existing  $\Delta$  in the nucleus by looking for a  $\Delta^{++}$  in the final state which has been knocked out by the incident photon. The  $\Delta^{++}$  is the best choice, since it couples strongly to the photon—the cross section for the  $\Delta^{++}$  is six times larger than that for the  $\Delta^+$  [Lip87]—and the ratio of the probabilities of finding charged-Delta states in  ${}^3\text{He}$  is  $P(\Delta^{++}nn):P(\Delta^+np) = 3:2$ . Most important, the  $\Delta^{++}$  cannot be photoproduced on a nucleon in a single-step process (by simple charge conservation), so that the main background to our signal can arise only from a two-step process, in which an intermediate  $\pi^+$  (or  $\Delta^+$ ) that is photoproduced on one of the protons scatters from the second proton and forms a  $\Delta^{++}$ .

Since the  $\Delta^{++}$  has a very short lifetime, we detect its decay products,  $p$  and  $\pi^+$ , and reconstruct their missing mass and invariant mass. Using a small fraction of the  ${}^3\text{He}$  data, the former is shown in the top part of Fig. 9. The first peak, near the mass of the two neutrons, contains all the  $p\pi^+nn$  events, and the second structure seen at higher values is due to events having one or more additional pions in the final state. For photon energies below the threshold for an additional pion, our data are free of this background, as can be seen in the bottom part of Fig. 9. Since in all cases we are interested only in  $p\pi^+nn$  events, we cut out the events with missing mass below  $1.85 \text{ GeV}/c^2$  and above  $2.0 \text{ GeV}/c^2$ , and plot the invariant mass distribution of the remaining events, as shown in Fig. 10. One can see that most of the  $p\pi^+$  pairs result from  $\Delta^{++}$  decay, and for low photon energies we have a very clean  $\Delta^{++}$  signal, as can be seen in the bottom part of Fig. 10. We then further restrict the invariant mass of a good event to lie between  $1.0$  and  $1.35 \text{ GeV}/c^2$ , to reduce the backgrounds at higher photon energies as well.

In order to separate the  $\Delta^{++}$  knockout events from those formed in a two-step process, we make use of the fact that most of the preformed Deltas in the nucleus are in an  $L = 2$  state relative to the  $nn$  pair, as required by isospin, angular momentum, and parity conservation [Str87]. Thus, their momentum and angular distributions are very

different from those of the two-step Deltas: the momentum distribution of the knockout Deltas should be strongly peaked, whereas that of the two-step Deltas should be broadly distributed, and the two-step Deltas should be more forward peaked than the knockout Deltas. Figure 11 shows the momentum distributions for our two lowest energy bins, showing considerable peaking.

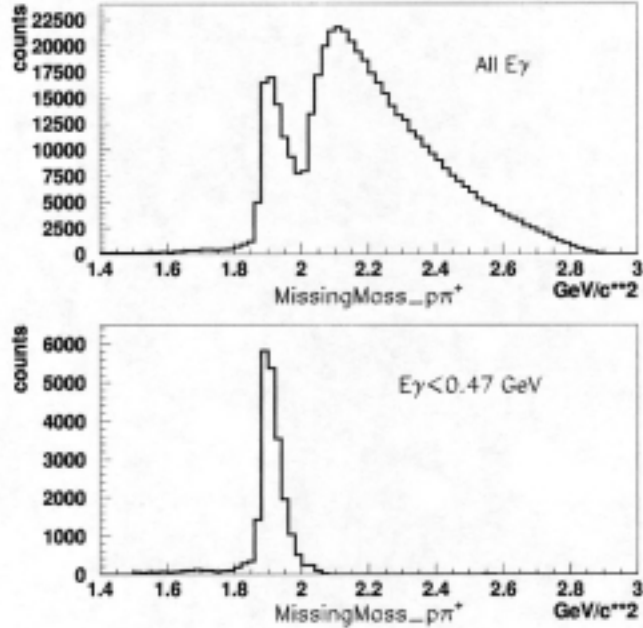


Figure 9. Missing-mass plots for detected  $p\pi^+$  coincident pairs from  ${}^3\text{He}$ , for (top) all photon energies and (bottom) photon energies below 0.47 GeV. The first peak corresponds to the mass of two neutrons.

At higher photon energies, the analysis is complicated by the backgrounds from multipion and high-invariant-mass events. The former can be suppressed by background subtraction for each  $(E_\gamma, \theta_\Delta, p_\Delta)$  bin, using the missing-mass distribution, and the latter can be suppressed by use of an additional cut on the  $p_p$  vs  $p_\pi$  correlation spectrum at fixed  $\Delta^{++}$  momentum.

We propose to use the same analysis technique for measuring the  $\Delta^{++}$  component in the  ${}^{12}\text{C}$  ground-state wave function in the same tagged-photon energy range as for  ${}^3\text{He}$  and  ${}^4\text{He}$ . This range is optimal, since it gives us access to two distinct regions of excitation energy: for the lower part of the spectrum, where the two-step process might be significant, the data are very clean, while for the upper part, where the multipion and non-Delta backgrounds are large, the contamination from two-step processes is expected to be much smaller.

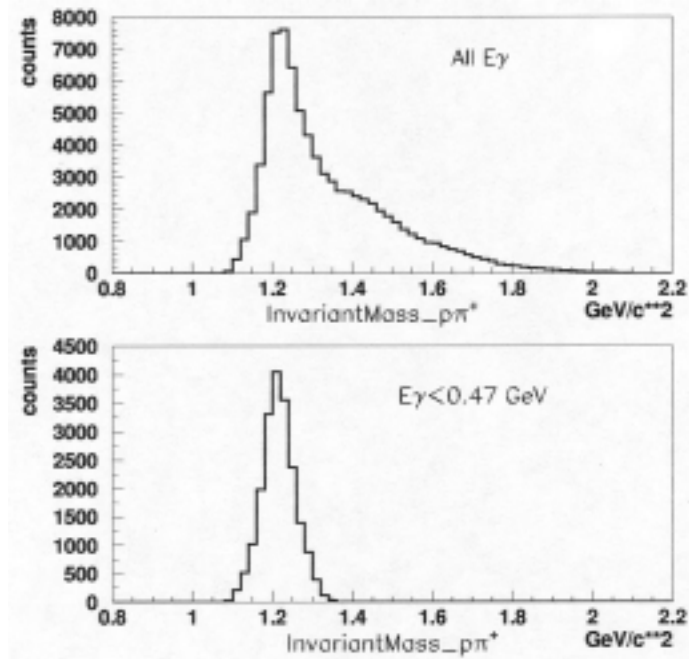


Figure 10. Invariant-mass plots for detected  $p\pi^+$  coincident pairs from  ${}^3\text{He}$ , for (top) all photon energies and (bottom) photon energies below 0.47 GeV, showing that most (top) and nearly all (bottom) of the events correspond to the mass of the  $\Delta^{++}$ .

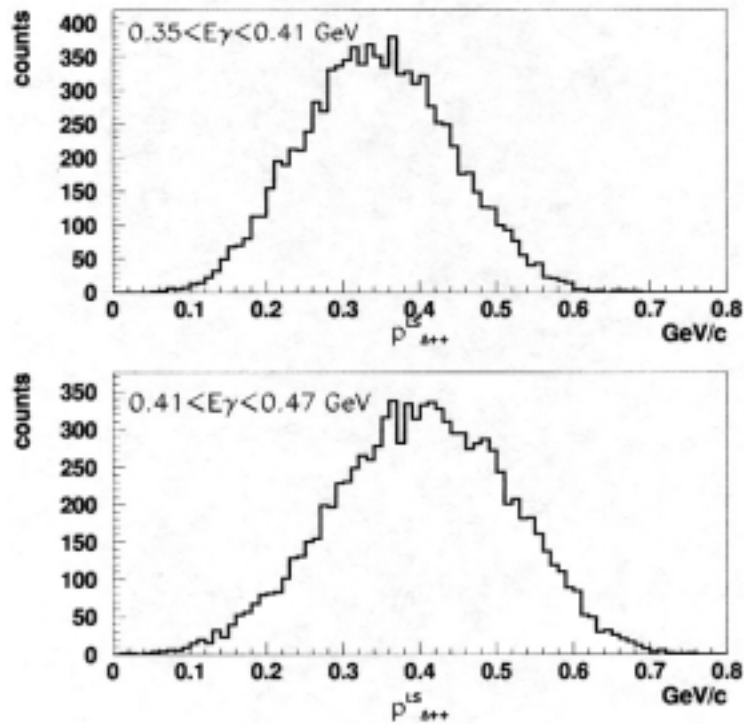


Figure 11. Momentum distribution of the emitted  $\Delta^{++}$ s, for photon-energy bins centered at (top) 0.38 GeV and (bottom) 0.44 GeV, showing peaked distributions.

It has been suggested [Hor78] that heavy nuclei are more appropriate for the study of internal nucleon excitations, since their higher relative two-nucleon density is expected to lead to larger isobar-configuration effects. This calculation, performed with a nonrelativistic perturbative approach, predicts a 3.2% probability for isobar configurations in the ground state on  $^{16}\text{O}$ . Recent work [Wri98] based on the same approach discusses the probability of finding  $\Delta^{++}$  excitations in single-particle orbitals in  $^{12}\text{C}$  and the effects resulting from their knockout on experimental observables, including differential cross sections and photon asymmetries. In particular, the differential cross section is predicted to be more peaked for  $\Delta^{++}$  knockout from S orbitals than from P orbitals. Therefore, for  $^{12}\text{C}$ , in addition to the cuts we employ for the  $^3\text{He}$  data, we will also construct the missing-energy spectrum  $E_m = E_\gamma - T_\pi - T_p - T_r$ , where the first three terms on the right are the photon, pion, and proton energies and the last term is the kinetic energy of the residual  $^{11}\text{Be}$  nucleus obtained from its reconstructed momentum. The energy resolution of the CLAS will allow us to separate the peaks in this spectrum corresponding to  $\Delta^{++}$  knockout from S and P orbitals.

Within another model for Delta knockout from  $^{12}\text{C}$ , also based on the impulse approximation, the elementary  $\gamma\Delta^{++} \rightarrow p\pi^+$  amplitude is calculated and then embedded into the nuclear system [Fix99]. The particular interest in studying the  $\Delta$ -isobar admixture in the  $^{12}\text{C}$  ground state was stimulated by a measurement of  $\gamma^{12}\text{C} \rightarrow p\pi^+$  at MAMI [Lia97]. The Valencia Model [Car92], which was developed to describe medium effects and final-state interactions in reactions on complex nuclei, but which does not take into account the isobar component of the nuclear wave function, fails to explain the magnitude and shape of the  $p\pi^+$  differential cross sections. A comparison of both model calculations [Wri98] and [Fix99] with these data, under the assumption that all  $p\pi^+$  pairs are decay products of knocked-out Deltas, shows a relatively good agreement, and indeed illustrates the important role of Delta internal degrees of freedom in nuclei. Both stress the need for true exclusive data, of the kind we can obtain with the CLAS, in order to separate the FSI background from the knockout process.

The only direct measurement of Delta knockout from  $^{12}\text{C}$  [Bys02] has been done in a very limited kinematic region and has produced only 53  $p\pi^+$  events, of which 13 are thought to be true knockout events. Therefore, the extracted number of Delta per nucleon, 0.017, has a large uncertainty and is not conclusive. There are several reports in the literature of experimental evidence for a  $\Delta$  component in the ground state of nuclei, from  $^3\text{H}$  to  $^{208}\text{Pb}$ , from pion double-charge exchange [Mor82], [Mor98], [Pas02] or proton-induced knockout [Ame94]. The resulting  $\Delta$  probabilities range from 0.5% to 3%, but all have been extracted by indirect means and therefore they, too, have large experimental uncertainties. Our proposed direct measurement of  $\Delta^{++}$  knockout by photons should resolve the issue of the  $\Delta$  components in the nuclear wave function as functions of both nuclear density and nuclear size.

The expected counting rates for this channel will be much higher than those for either kaon or eta production.

## Other Reaction Channels

Although the principal photoreaction channels we propose to pursue are delineated above, we also intend to study, with lower priority, a number of other channels, as given below. Some of these have their counterparts in Experiment 93-044, some have arisen from other analyses in which we have been engaged. We anticipate that still others, not listed below, will become targets of opportunity when we analyze the g3b data.

### *Rho production and mass modification (N. Benmouna)*

A current topic of great interest is the modification of the mass, and perhaps the width, of the rho, and perhaps other vector mesons, in the nuclear medium. Indeed, the entire g7 experiment [Wey01] has as its goal the delineation of this phenomenon, predicted by theories of chiral-symmetry restoration [Rap99] to be a density-dependent effect that should be observable at ordinary nuclear densities. Although it is widely thought that the lightest nuclei would be the best candidates for seeing this phenomenon, Thomas has stated [Tho98] that “a comparison with data on a slightly heavier nucleus such as  $^{12}\text{C}$  would also be useful.”

We have been analyzing the  $\pi^+\pi^-$ -production channel on  $^3\text{He}$  from the g3a data, to see if we could isolate such events that arise from the decay of the  $\rho^0$ . In fact, it turns out that this analysis is very straightforward, and the rho-decay events can be separated from much of the background by a series of simple cuts. The top part of Fig. 12 shows missing-mass plots for all the  $\pi^+\pi^-$  events (solid curve) and for those events corresponding to photon energies below and above 0.9 GeV (heavy dots and light dots, respectively), each of which has a distinct peak at the three-nucleon mass. For events with incident photon energies above the rho threshold, this peak is more pronounced. When the invariant mass of these events is plotted, in the bottom part of Fig. 12, one sees, for all the events, a distinct rho peak atop a background; and when one examines the invariant-mass distributions of the  $\pi^+\pi^-$  events from photon energies below and above 0.9 GeV, one finds that most of the background events are concentrated in the lower part and most of the rho events in the upper part. Of course, since these pions scatter strongly from the other nucleons in the nucleus, one must analyze and fit the data very carefully before concluding that any evidence exists for medium modification of the rho mass. But  $^3\text{He}$  is mostly surface (as is  $^4\text{He}$ ), so that when this distribution is compared with what we will see from  $^{12}\text{C}$ , which has “interior” S-shell nucleons and “exterior” P-shell nucleons, and from Pb, which is mostly volume and relatively less surface (roughly in the ratio 3:1 [Ber75]), we may be able to infer to what extent any observed mass shift may be due to the effect of the nuclear medium. In other words, if the mass shift of the rho were density-dependent and the final-state interactions were size-dependent, we would hope to be able to separate them by comparing the data from g3a ( $^3\text{He}$  and  $^4\text{He}$ ) with those from g3b ( $^{12}\text{C}$  and Pb).

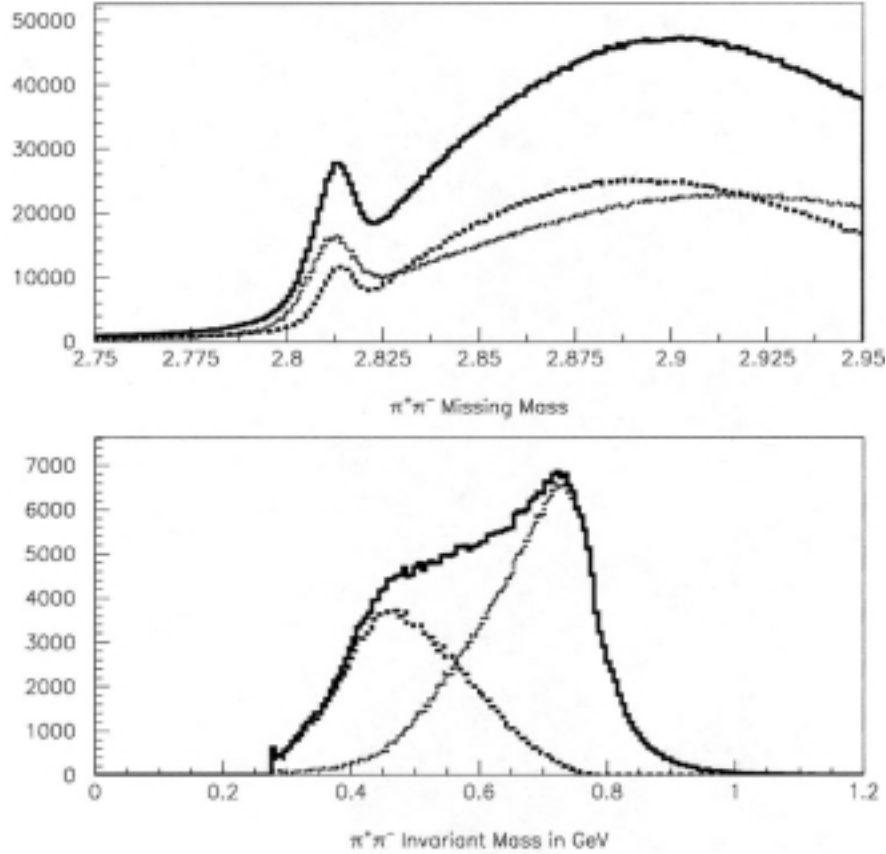


Figure 12. The top panel shows the missing-mass distribution for  $\pi^+\pi^-$  events from  ${}^3\text{He}$ ; the bottom panel shows the invariant mass distribution for those events with missing mass in the interval  $2.80 - 2.82 \text{ GeV}/c^2$ . For both panels, the solid curves correspond to all photon energies, while the heavy-dotted and light-dotted curves correspond to photon energies below and above  $0.9 \text{ GeV}$ . The latter distribution is dominated by  $\pi^+\pi^-$  events from  $\rho^0$  decay.

### ***Delta-pi and nucleon-rho branching ratio from decay of $N^*$ s (N. Benmouna)***

In our analysis of the  $p\pi^0\pi^0$  channel in the g1 data [Phi02], we found strong evidence, in the invariant-mass plots, for decay of an  $N^*$  having  $W = 1700 \text{ MeV}$  into the  $\Delta-\pi$  channel, shown in Fig. 13, and weaker evidence for decay into the  $D_{13}-\pi$  channel. We therefore believe that we can identify, under favorable conditions, such branching ratios, including that for the  $N-\rho$  channel. The evidence would come from analysis of  $p\pi^+\pi^-$  events, where in the one case, the invariant mass of the  $p\pi^-$  would reconstruct to that of the  $\Delta^0$ , while in the other, the invariant mass of the  $\pi^+\pi^-$  would reconstruct to that of the  $\rho^0$ . Whether such branching ratios would be density- or size-dependent is currently a matter for speculation, but even used simply as a tool for determining whether and to what extent  $N^*$ s, especially so-called “missing”  $N^*$ s that do not couple strongly to  $N\pi$ , are excited in nuclei, such observations would break new ground.

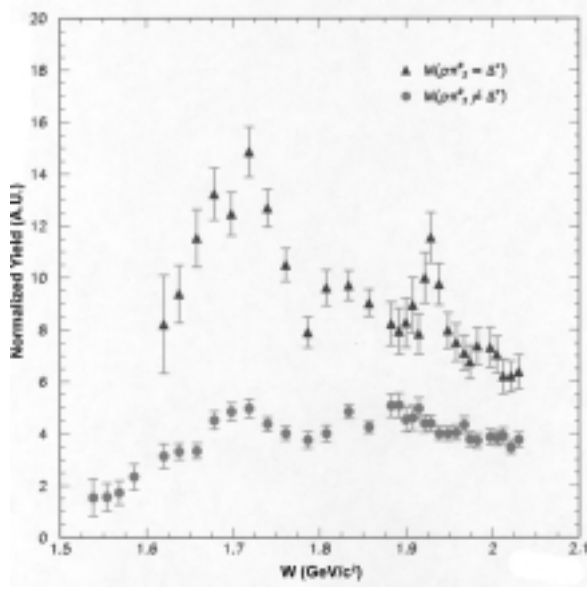


Figure 13.  $W$ -distribution for  $p\pi^0\pi^0$  events that decay through the  $\Delta^+-\pi^0$  channel, showing that the probability for decay of an  $N^*(1700)$  through this channel is about 75%.

### *Asymmetries from circularly polarized photons (S. Strauch)*

The g3a data were obtained with circularly polarized photons on unpolarized targets. We have been analyzing the  $^3\text{He}$  single- and double-charged-pion channels for polarization effects, and in fact we have been able to find very large asymmetries in the helicity-dependent cross section. This asymmetry constitutes a new observable and is only accessible in reactions with more than two particles in the final state. Owing to the large angular acceptance of the CLAS, nearly complete angular distributions of the cross-section asymmetries can be measured. Figure 14 shows preliminary results for the  $\pi^+\pi^-$  channel and two different photon-energy bins as a function of the relative azimuthal angle of the two pions in the laboratory frame. They are strikingly different.

We also have compared the asymmetries for  $^3\text{He}$  with those for the proton (from g1 data), as shown in Fig. 15. Here the top and bottom panels show different Fourier components of the observed angular distributions. The asymmetry has been corrected for the energy-dependent polarization of the photon beam [Max02]. For a better comparison, the smaller asymmetries for  $^3\text{He}$  were scaled to match the (larger) asymmetries for the proton. We notice not only that these asymmetries are very large, but that their dependence on incident photon energy is strikingly different, showing the existence of nuclear effects not seen on the nucleon. Currently, we are attempting to correlate these asymmetries with various reaction channels (such as  $\rho^0$  decay). Nevertheless, these effects are large, and we should be able to observe them in  $^4\text{He}$  and  $^{12}\text{C}$ , and perhaps even in Pb (if they are present in these nuclei). A comparison of these large effects as a function of both nuclear size and density will surely be illuminating.

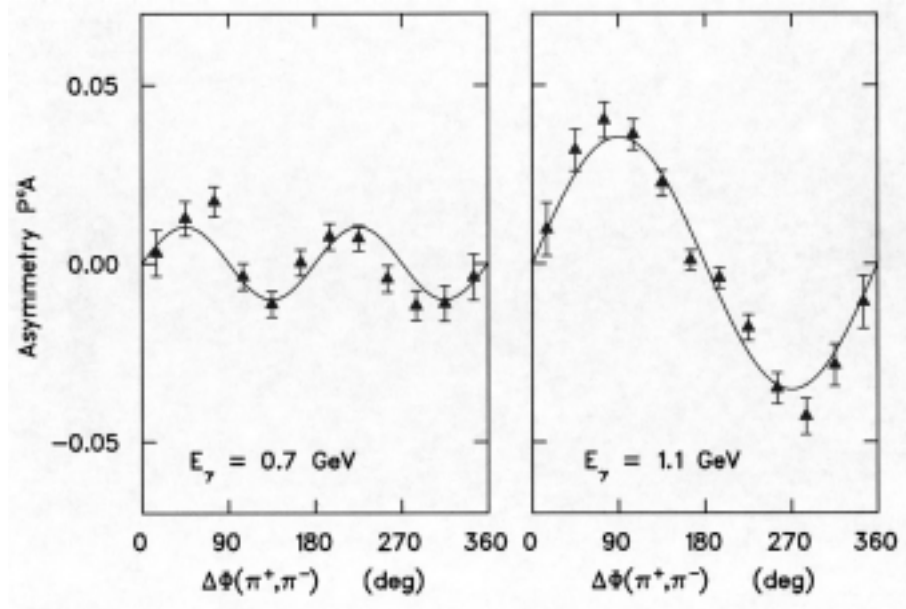


Figure 14. Angular distribution for two photon-energy bins of the polarization-dependent part of the cross section for the photoproduction of  $\pi^+\pi^-$  events from  ${}^3\text{He}$ .

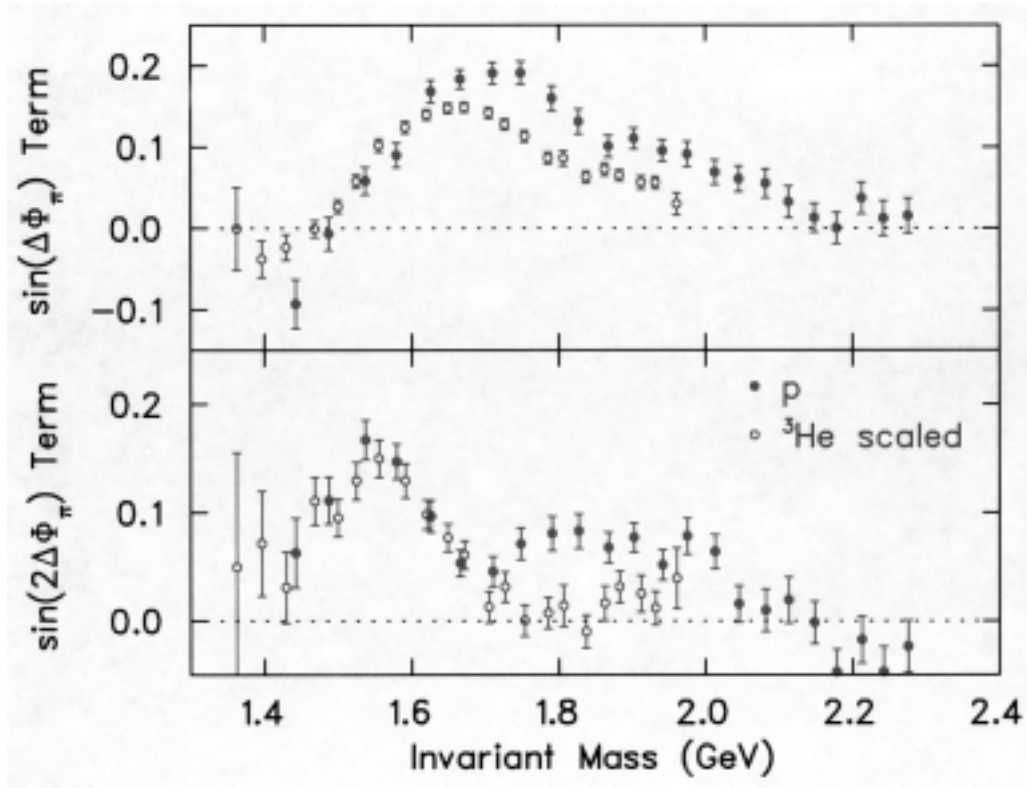


Figure 15. Fourier components of the cross-section asymmetry in the photoproduction of  $\pi^+\pi^-$  events from  ${}^3\text{He}$ , as a function of incident photon energy for circularly polarized photons, compared with corresponding data for the proton.

### ***Total photonuclear cross section (P. Heimberg)***

The Frascati group, in total photonuclear absorption experiments at both Frascati and Bonn, have recently published data for nuclei including both  $^{12}\text{C}$  and Pb which have shown an almost featureless cross section in the region of the  $D_{13}$  and  $F_{15}$  resonances that are seen prominently in the proton and deuteron [Muc99]. However, their method, which consists basically of identifying large-angle events with hadronic and small-angle events with electromagnetic interactions, is open to some experimental uncertainties. Their data, which they claim to show the *disappearance* (quenching, not merely broadening) of photon absorption strength in nuclei heavier than the helium isotopes, calls for verification by another technique. CLAS provides us with a unique opportunity to test these results, since for a nucleus having  $Z$  as large as 6, enough charged particles would be emitted so that nearly all photonuclear events would be detected. In other words, the experimental efficiency would be very high, the acceptance correction to the raw data would be very small, and the total photonuclear cross section would be easy to determine.

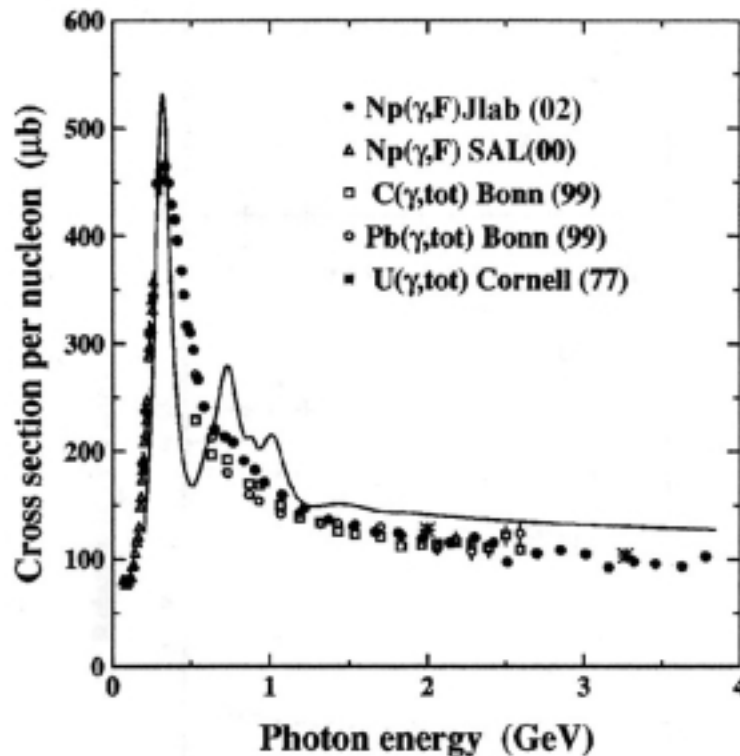


Figure 16. Photoabsorption data for C and Pb from Bonn [Muc99], compared with the photofission cross section per nucleon for Np and earlier photoabsorption data for U and the proton (continuous curve) (from [Cet02]).

## Target and Beam-Time Considerations

### *Number and thickness*

We intend to use six graphite foils, each 0.5 mm thick, and one lead foil 0.3 mm thick. This gives a total target thickness of about  $1 \text{ g/cm}^2$ , with the nuclear samples in the ratio of roughly  $^{12}\text{C}:\text{Pb} = 2:1$ . They can be mounted as in the g7 experiment, or perhaps in a hexagonal slotted-rod arrangement that results in even less material between the target foils and the active areas of the CLAS. Since no super-insulation will be needed, the backgrounds (and energy loss) from material surrounding the target samples should be even lower than for the g3a run.

### *Energy loss*

A 25-MeV proton loses about 3 MeV in 0.3 mm of Pb. Its range in Pb is about 1.6 mm, about five times the thickness of our proposed lead foil. For the graphite foils, the numbers are even more favorable. If the spacing of the foils were 3 cm, then the total extension along the beam line of the seven foils would be 18 cm, about the thickness of the g3a cryogenic targets. If the diameter of the foils were also about 3 cm, they would comfortably intercept most of the beam, even with no collimation ( $mc^2/E_e = 0.3 \text{ mrad}$  for  $E_e = 1.6 \text{ GeV}$ , so that the half-intensity photon beam diameter at the position of the target samples is about 1.5 cm). [Collimation will be used to eliminate any beam halo.]

### *Beam time*

We intend to use essentially the same running conditions as were used for g3a: a level-two single-charged-particle trigger plus about 10% double-neutral trigger, and an electron beam energy of about 1.6 GeV. The electron beam current will be adjusted to give a tagged-photon flux of about  $2 \times 10^7 \text{ s}^{-1}$  (about 15 nA incident on a radiator  $5 \times 10^{-4}$  r.l. thick). With this flux, a target thickness of about  $1 \text{ g/cm}^2$  would result in a total counting rate of about 3 kHz (the mean total photonuclear cross section being about  $250 \text{ } \mu\text{b/nucleon}$  in the energy range between 0.3 and 1.5 GeV). In six days (150 hours) of data-taking time, allowing for about 10 hours of normalization runs, we should obtain about  $10^9$  events for  $^{12}\text{C}$  and about half that many for Pb.

## References

- [Abu00] L.J. Abu-Raddad and J. Piekarewicz, Phys. Rev. C **61**, 014604 (2000)
- [Ame94] A.I. Amelin *et al.*, Phys. Lett. **B337**, 261 (1994)
- [Ben98] C. Bennhold *et al.*, Nucl. Phys. **A639**, 209 (1998)
- [Ber75] B.L. Berman and S.C. Fultz, Rev. Mod. Phys. **47**, 713 (1975)
- [Bys02] V.M. Bystritsky *et al.*, nucl-ex/0112013 (2002)
- [Car92] R. Carrasco and E. Oset, Nucl. Phys. **A536**, 445 (1992)
- [Car93] R.C. Carrasco, Phys. Rev. C **48**, 2333 (1993)
- [Cet02] C. Cetina *et al.*, Phys. Rev. C **65**, 044622 (2002)
- [Chi91] H.C. Chiang, E. Oset, and L.C. Liu, Phys. Rev. C **44**, 738 (1991)
- [Chr88] R.E. Chrien *et al.*, Phys. Rev. Lett. **60**, 2595 (1988)
- [Dov91] C.B. Dover and D.J. Millener, *Electroproduction of Strangeness*, World Scientific (1991)
- [Dug02] M. Dugger *et al.*, *Eta Photoproduction on the Proton for Photon Energies from 0.75 to 1.95 GeV*, in preparation (2002)
- [Eff97] M. Effenberger *et al.*, Nucl. Phys. **A614**, 501 (1997)
- [Fix99] A. Fix *et al.*, Nucl. Phys. **A646**, 417 (1999)
- [Gre96] A.M. Green, J.A. Niskanen, and S. Wycech, Phys. Rev. C **54**, 1970 (1996)
- [Hai86] Q. Haider and L.C. Liu, Phys. Lett. **B172**, 257 (1986)
- [Hed98] M. Hedayati-Poor and H.S. Sherif, Phys. Rev. C **58**, 326 (1998)
- [Hor78] G. Horlacher and H. Arenhövel, Nucl. Phys. **A300**, 348 (1978)
- [Hyd91] C.E. Hyde-Wright *et al.*, *Quasi-Free Strangeness Production in Nuclei* (1991)
- [Lee96] F.X. Lee *et al.*, Nucl. Phys. **A603**, 345 (1996)
- [Lee01] F.X. Lee *et al.*, Nucl. Phys. **A695**, 237 (2001)
- [Lia97] M. Liang *et al.*, Phys. Lett. **B411**, 244 (1997)
- [Lie89] B.J. Lieb *et al.*, Int. Nucl. Phys. Conf., São Paulo (1989)
- [Lip87] H.J. Lipkin and T-S. H. Lee, Phys. Lett. **B183**, 22 (1987)
- [Max02] L.C. Maximon, private communication (2002)
- [Mor82] C.L. Morris *et al.*, Phys. Rev. C **25**, 3218 (1982)
- [Mor98] C.L. Morris *et al.*, Phys. Lett. **B419**, 25 (1998)
- [Muc99] V. Muccifora *et al.*, Phys. Rev. C **60**, 064616 (1999)
- [Nic02] I. Niculescu *et al.*, nucl-ex/0108013 (2001)
- [Pas02] E.A. Pasyuk *et al.*, Phys. Lett. **B523**, 1 (2002)
- [Phi02] S.A. Philips, Ph.D. thesis, The George Washington University (2002)
- [Rak96] S.A. Rakityansky *et al.*, Phys. Rev. C **53**, 2043 (1996)
- [Rap99] R. Rapp and J. Wambach, hep-ph/9909229 (1999)
- [Roe96] M. Roebig-Landau *et al.*, Phys. Lett. **B373**, 45 (1996)
- [Sib01] A. Sibirtsev, W. Cassing, and U. Mosel, Nucl. Phys. **A679**, 497 (2001)
- [Sok01] G.A. Sokol, A.I. L'vov, and L.N. Pavlyuchenko, NSTAR2001, Mainz (2001)
- [Str87] W. Strüve *et al.*, Nucl. Phys. **A465**, 651 (1987)
- [Tho98] A. Thomas, Nucl. Phys. **A629**, 20c (1998)
- [Tra98] M.Q. Tran *et al.*, Phys. Lett. **B445**, 20 (1998)
- [Wey01] D.P. Weygand *et al.*, *Photoproduction of Vector Mesons off Nuclei* (2001)
- [Wil93] C. Wilkin, Phys. Rev. C **47**, 938 (1993)

- [Wri98] L.E. Wright and C-H. Chang, in *Electronuclear Physics with Internal Targets and the BLAST Detector*, Cambridge (1998)
- [Wyc95] S. Wycech, A.M. Green, and J.A. Niskanen, *Phys. Rev. C* **52**, 544 (1995)
- [Yam95] H. Yamazaki *et al.*, *Phys. Rev. C* **52**, 1157 (1995)
- [Yor00] T. Yorita *et al.*, *Phys. Lett.* **B476**, 226 (2000)
- [Zei01] B. Zeidman *et al.*, *Nucl. Phys.* **A691**, 37 (2001)

## **Appendix: Auxiliary Information**

### ***Experiments with similar physics goals***

Several aspects of the e2 group of experiments are complementary to those outlined here; e2 constitutes, in some sense, the electron-scattering counterpart to the g3 photon measurements. This is quite intentional, since these two groups of experiments are the principal Hall-B contributions to nuclear physics.

The g7 experiment is exclusively concerned with the modification of vector mesons in the nuclear medium, but uses a different method (detection of the  $e^+e^-$  pair from rho decay) and consequently a much-restricted trigger.

We were unable to identify any overlapping experiments in Hall A or Hall C except for 91-006 (Hall A) which bears a distant relationship in that it also seeks to uncover medium effects in nuclei, including  $^{12}\text{C}$ .

### ***Computational resources***

As we have done for the g3a data, we intend also to bring the g3b data to GW for analysis on our minifarm/minisilo facility. We would hope to do this as soon as the data acquisition has been completed. This places a minimum of requirements on the JLab computational facilities.

### ***Requested time of run***

We hope to run this experiment in the second half of 2003. It is short, and other than a few days for target construction, requires no special or large-scale preparations of equipment or software.

***Copies of original g3 proposals and updates are available on demand***